LETTERS TO THE EDITOR

This Letters section is for publishing (a) brief acoustical research or applied acoustical reports, (b) comments on articles or letters previously published in this Journal, and (c) a reply by the article author to criticism by the Letter author in (b). Extensive reports should be submitted as articles, not in a letter series. Letters are peer-reviewed on the same basis as articles, but usually require less review time before acceptance. Letters cannot exceed four printed pages (approximately 3000–4000 words) including figures, tables, references, and a required abstract of about 100 words.

Characterization of acoustic emissions resulting from particle collision with a stationary bubble (L)

Wen Zhang[a)]
Research School of Engineering, College of Engineering and Computer Science, The Australian National University, Building 115, Corner North and Daley Roads, Canberra, Australian Capital Territory 0200, Australia

Steven J. Spencer and Peter Coghill
Process Science and Engineering, Commonwealth Scientific and Industrial Research Organization, Lucas Heights Science and Technology Centre, New Illawarra Road, Lucas Heights, New South Wales 2232, Australia

(Received 28 September 2012; revised 31 January 2013; accepted 5 March 2013)

The present work characterizes the acoustic emissions resulting from the collision of a particle driven under gravity with a captive bubble. Conventional methods to investigate the bubble particle collision interaction model measure a descriptive parameter known as the collision time. During such a collision, particle impact may cause a strong deformation and a following oscillation of the bubble–particle interface generates detectable passive acoustic emissions (AE). Experiments and models presented show that the AE frequency monotonically decreases with the particle radius and is independent of the impact velocity, whereas the AE amplitude has a more complicated relationship with impact parameters. © *2013 Acoustical Society of America*.
[http://dx.doi.org/10.1121/1.4796124]

PACS number(s): 43.30.Jx, 43.20.Ye [TK] Pages: 2523–2527

I. INTRODUCTION

The flotation process is an effective separation method to extract various particulate solids from water. Its industrial applications are enormous, such as separating valuable minerals in the mining industry, waste water treatment, and deinking in paper recycling. Gas bubbles play a vital role in the flotation process to collect solid particles through two kinds of interactions between a particle and a bubble: the collision interaction and the sliding interaction. This paper focuses on characterizing the bubble–particle collision interaction, where a particle approaches a stationary bubble in a straight line.

During the bubble–particle collision involving relative high kinetic energy of interaction, the bubble wall is strongly deformed in the region of the particle and a following oscillation of the local bubble surface occurs. The elasticity here is due to the interfacial tension or as a result of the minimizing of free surface energy. A key descriptive parameter is the collision contact time between a bubble and a particle, τ_c, which is defined in the literature as the half period of the oscillation during particle impact.[1] A variety of analytical models have been developed to predict the collision time[2–6] between a spherical particle and a gas bubble. An assumption adopted in these models is that the bubble size is much larger than the particle size so the collision interaction has been approximated as a spherical particle against a planar gas–liquid interface. Deformation of the gas–liquid surface due to the impact of a spherical particle was treated initially as the shape of the spherical particle[2,5] and later modified to a smooth profile.[3,4,6] Experimental studies have been made using high-speed or stroboscopic photographic recordings of the bubble–particle collision interaction, where a particle was dropped onto a captive bubble formed on the top of a capillary.[4,7,8] Because the collision interaction is a process of limited time duration (around several ms), photographic techniques can still be problematic in terms of detecting/characterizing the oscillation. For example, the measured collision times are about 15% longer than the calculated times.[1]

Another promising technique to detect and characterize the bubble–particle collision interaction is acoustic monitoring. This technique has been shown very effective for short-time process characterization, given its capability of high time resolution sampling at a relatively low cost. Strong deformation of a bubble surface during a collision interaction involving significant kinetic energy can generate detectable sound. While

a)Author to whom correspondence should be addressed. Electronic mail: wen.zhang@anu.edu.au

the pressure changes inside the gas bubble during the particle impact have been studied by Wierink *et al.*;[9] to our best knowledge, the current work is the first to derive analytical formulas linking acoustic emissions (AE) and bubble– particle collision characteristics and to make confirmatory experimental measurements of the AE generated by a collision.

The AE frequency is the same as that of the bubble surface oscillation, which can be used to estimate the key descriptive parameter, the collision time (half of the reciprocal of the AE frequency). The local bubble deformation is here treated as a point sound source and the magnitude of its induced pressure fluctuations in the nearby water is related to the bubble deformation depth. Passive AE information not only provides accurate estimates of the key parameters in the bubble–particle collision interaction but also, based on the same principle, may be applied to more complicated systems where multiple particles and bubble swarms are present and associated.

II. THEORETICAL DEVELOPMENT

A. Physics of the collision process

In flotation, the bubble size is usually much larger than the particle size.[1] In this case, we can reasonably assume that an idealized physical picture of a collision interaction as the deformation of a planar gas–liquid interface by an approaching spherical solid particle, as shown in Fig. 1. The gas–liquid interface will deform smoothly as shown by Scheludko *et al.*[3] Therefore, the deformation interface could be modeled as composed of two parts (Fig. 1).[3,4] The first part is a thin liquid film (spherical cap) with radius R_m, over which there is a strong hydrodynamic interaction between bubble and particle (corresponding depth of deformation h_1). The second part is a free surface over which only weak interaction exists between bubble and particle (corresponding depth of deformation h_2).

Since the bubble surface is deformable, particle impact causes a compression and then a following oscillation of the local bubble surface. Even though the particle slides down on the bubble wall right after the collision, it has been proven that the collision process and the following sliding process are of almost the same frequency.[4]

In this paper, the general equation of motion adopted to describe the initial compression and the subsequent bubble–particle interface oscillation is as follows:

$$m_{\text{eff}}\ddot{h} + F_D(\dot{h}) + F_R(h) = m_p\left(1 - \rho_\ell/\rho_p\right)g. \tag{1}$$

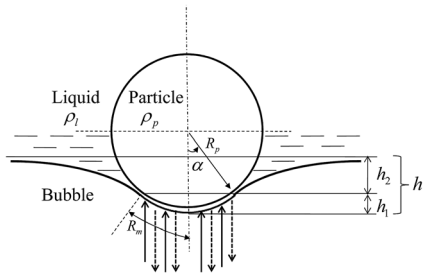

FIG. 1. Deformation of bubble surface during collision of a spherical particle.

Here h, $\dot{h}$, and $\ddot{h}$ are the local deformation, its velocity and acceleration, respectively; $m_p = \frac{4}{3}\pi R_p^3\rho_p$ is the mass of particle, where R_p and ρ_p are particle radius and density; g is the acceleration of gravity; m_{eff} is the effective mass of oscillation and is generally represented as

$$m_{\text{eff}} = m_p(1 + j\rho_\ell/\rho_p), \tag{2}$$

i.e., the mass of particle and the co-oscillating liquid adjacent to the particle. The value of j depends on the frequency of the impacting particle and in most cases $j = 1.5$ is chosen for calculation.[4] It has been shown that the second term in Eq. (2) explains the non-steady resistance of liquid to an oscillating interface and has very little effect on the frequency of oscillation or collision time.[6] In this work, we adopt the following relation that $m_{\text{eff}} \approx m_p$.

The term $F_D(\dot{h})$ is the damping force due to viscous dissipation, thermal damping, and wave energy radiation and depends on the oscillation rate $\dot{h}$. $F_R(h)$ is the restoring force and ideally should be represented as a function of the deformation depth, i.e., $F_R(h) = kh$ (Hooke's Law[10]), where the parameter k is the stiffness (or spring constant) of the oscillation. In the present work, we investigate a particle moving under gravity colliding with a stationary bubble and thus can assume a constant external force due to the action of gravity (taken into account of buoyancy), $m_p(1 - \rho_\ell/\rho_p)g$, where ρ_ℓ is the liquid density.

Equation (1) is the classical equation of motion of a damped harmonic oscillator and has well-known properties and analytical solutions.[11] For example, the local bubble surface oscillation can be represented in the following form:

$$h = h_0 e^{-bt} e^{iw_0 t}, \tag{3}$$

where h_0 is the maximum deformation depth, w_0 is the angular frequency, i.e., $f_0 = w_0/(2\pi)$ is the oscillation frequency, and b is the damping (or dissipation) constant. The wave energy radiation is expected to be a dominant term in the damping force, which is directly related to the shape of the local bubble surface deformation formed by particle impact and remains unsolved in the framework of the present study. Additionally, we are not interested in the time to the steady state. Therefore, we have neglected in the first approximation of modeling the gas–liquid interface oscillation of the damping behavior. The damping constant in Eq. (3) is set to a nil value.

1. Equilibrium state

The deformation depth at equilibrium state can be written as

$$h_e = h_{1e} + h_{2e} \tag{4}$$

with the spherical cap thin liquid film depth

$$h_{1e} = R_p(1 - \cos\alpha_{\text{eq}}), \tag{5}$$

and the depth of the equilibrium meniscus with axial symmetry in a gravitational field[12]

$$h_{2e} = R_p \sin^2\alpha_{\text{eq}} \ln\left[e^{-\gamma}\frac{\sqrt{16\sigma/R_p^2\rho_\ell g}}{(1+\cos\alpha_{\text{eq}})\sin\alpha_{\text{eq}}}\right]. \quad (6)$$

Here, γ is the Euler number (0.5772). The angle α_{eq} is associated with the half-arc length of the thin layer at equilibrium, and σ is the surface tension coefficient (assumed constant).

The value of the angle α_{eq} can be obtained from a force balance at equilibrium state. In this case, the restoring force acting on the particle is the capillary force resulting from the curved liquid/gas interface, $F_s = -2\pi\sigma R_p \sin^2\alpha_{\text{eq}}$; then the balance of the gravity and bubble deformation restoring force gives

$$|F_s| = |\bar{m}_p g|, \quad (7)$$

where $\bar{m}_p = m_p(1-\rho_\ell/\rho_p)$; and

$$\alpha_{\text{eq}} \approx R_p\sqrt{2(\rho_p-\rho_\ell)g/3\sigma} \quad (8)$$

as $\alpha_{\text{eq}} \ll 1$ is assumed so that $\sin\alpha_{\text{eq}} \approx \alpha_{\text{eq}}$. Hence, provided the size of the particle, the density of the particle and liquid, and the surface tension are known, the equilibrium deformation depth can be determined.

The stiffness of the oscillation can then be found from the force balance at equilibrium state

$$k = \bar{m}_p g/h_e. \quad (9)$$

2. Maximum displacement state

The amplitude of the bubble–particle interface oscillation is here equated with the initial maximum deformation displacement due to the particle impact. It is here assumed that at the moment of the bubble–particle collision interaction the kinetic energy of impact transfers entirely to the local potential energy (modeled as a spring); hence, the maximum deformation depth can be obtained via

$$h_0 = \sqrt{m_p/k}V_t, \quad (10)$$

where $V_t = 2(\rho_p-\rho_\ell)gR_p^2/9\mu$ is the particle stokes settling velocity before the collision with μ being the dynamic viscosity of the liquid.

B. Acoustic emission models

We treat this oscillation as a monopole point acoustic source because the wavelength is much longer than the size of the bubble surface deformation. The frequency of acoustic emission is taken as equal to the frequency of oscillation of the bubble surface. Substituting Eq. (3) into (1) with the approximation $m_{\text{eff}} \approx m_p$, ignoring the damping term, and solving for the deformation depth leads to the following expression for the frequency of oscillation of the bubble surface,

$$f_0 = (1/2\pi)\sqrt{k/m_p} = (1/2\pi)\sqrt{(\rho_p-\rho_\ell)g/\rho_p h_e}. \quad (11)$$

The amplitude of acoustic emission is obtained from calculating the liquid mass flux caused by the bubble surface oscillation,

$$q(t) = \rho_\ell SU = \rho_\ell n\pi R_p^2 h_0 i w_0 e^{iw_0 t}, \quad (12)$$

where $S = n\pi R_p^2$ is the cross-sectional area of displaced liquid ($n = 0.5$ is assumed) and $U = ih_0 w_0 e^{iw_0 t}$, where $w_0 = 2\pi f_0$ is the velocity of oscillation.

We write

$$\varphi(t) = -q(t-r/c)/4\pi\rho_\ell r \quad (13)$$

as the velocity potential at distance r from this acoustic monopole point source.[13] The corresponding pressure fluctuation is

$$\tilde{p}(t) = -\rho_\ell \partial\varphi/\partial t = (\rho_\ell R_p^2 h_0 w_0^2/8r)e^{iw_0(t-r/c)}, \quad (14)$$

allowing the corresponding maximum AE amplitude to be identified as

$$A_0 = \rho_\ell R_p^2 h_0 w_0^2/8r. \quad (15)$$

III. EXPERIMENTAL METHODOLOGY

A schematic diagram of the experimental apparatus is shown in Fig. 2. A particle dropping technique[1,14] is adopted in the present work to build a particle–bubble collision apparatus, such that a particle driven under gravity falls onto a stationary bubble. The experiment is performed in quiescent liquid water ($\sigma = 71.97\,\text{mN/m}$, $\rho_\ell = 1000\,\text{kg/m}^3$) within a laboratory glass tank of 60 $\text{cm}^3 \times 60\ \text{cm}^3 \times 60\ \text{cm}^3$ volumetric capacity. Two different sizes of air bubbles (1 and 1.5 mm in radius) can be generated at the end of an L-shape stainless steel capillary (horizontally orientated) using a syringe attached to the other end of the capillary. An individual bubble is transferred to a plastic rod so that the bubble gas remains trapped during acoustic excitation. A range of different sizes of spherical hydrophobic glass spheres (from 250 or 600 μm in radius and density of 2800 kg/m^3) fall freely in the liquid through a guiding tube with an inner diameter of 2 mm positioned above the air bubble and subsequently collide with the stationary bubble.

Three Brüel and Kjær 8103 hydrophones (0.1–100 kHz frequency range) placed at three different positions (0.5, 1, and 1.5 cm) from the bubble–particle impact point are used with a

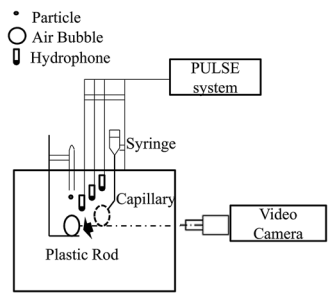

FIG. 2. Schematic diagram of the experimental apparatus.

Brüel and Kjær PULSE^{TM} platform to measure the acoustic response of the interaction. Meanwhile, the entire bubble–particle collision process is recorded using a MotionPro X3 high-speed video camera equipped with a Navitar Zoom 12× lens operating at 500 frames per second. Video images are subsequently processed using Image-Pro Plus 7.0 software to validate the particle settling velocity before interaction. Synchronization of acoustic measurements with high-speed photographic images is achieved so that the acoustic signature of the collision interaction can be unambiguously identified.

IV. RESULTS AND DISCUSSION

A. Acoustic emissions of collision process

Typical acoustic responses of a bubble–particle collision process are shown in Fig. 3. Particle impact on the bubble surface results in an oscillation of the bubble–particle interface, which can further induce a bubble shape oscillation (and detectable AE) depending on the particle kinetic energy.[15] The bubble–particle collision interaction is a strongly time-limited process (around several ms duration). Clearly, the damping forces are very strong for the bubble– particle interaction process investigated in these experiments. Again though, this does not strongly affect the frequency of bubble surface/AE oscillation or the maximum amplitude of the oscillation.

The acoustic measurements can show much higher resolution features of the process compared than high-speed photographic image recordings. In terms of estimating the key parameters for comparison of the AE model to the experiments, i.e., the frequency and maximum amplitude of the acoustic emissions, only the first two or three oscillations are relevant collision process. The AE amplitude spectrum is used to identify the frequency of the bubble surface oscillation process induced by the collision process. For example, for the AE responses of collision processes as shown in Figs. 3(a) and 3(b), the frequency peak at 40 Hz and 96 Hz, respectively, are

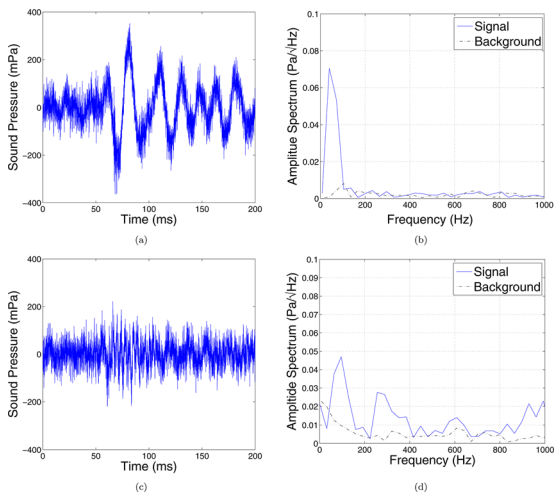

FIG. 3. (Color online) Acoustic emissions of a bubble–particle collision process. (a and b) AE response (time series and amplitude spectrum) of a particle of radius 600 μm colliding with a bubble of radius 1.5 mm at a distance of 1 cm away from the impact point. (c and d) AE response (time series and amplitude spectrum) of a particle of radius 300 μm colliding with a bubble of radius 1 mm at a distance of 0.5 cm away from the impact point. The corresponding AE frequencies of these collision processes are 40 Hz and 96 Hz, respectively.

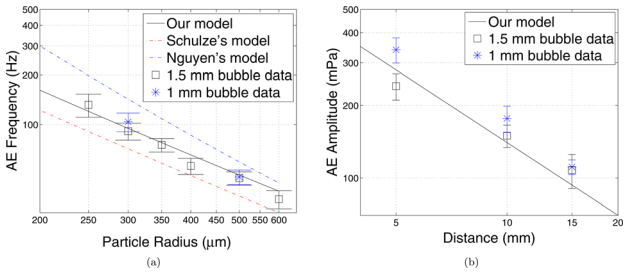

FIG. 4. (Color online) Comparison between the experimental data on the frequency and maximum amplitude of the acoustic emission and the theoretical predictions. (a) The log–log plot of the AE frequency versus the particle radius. (b) The log–log plot of the AE maximum amplitude versus the distance of the hydrophone position from the bubble particle impact point.

associated with collision of individual stationary bubbles with the particles of radius of 600 μm and 300 μm, respectively.

B. Characterization of collision process acoustic emissions

A comparison is made of the experimental data on the frequency and maximum amplitude of collision AE versus theory for bubble surface oscillations. The experimental data for the AE frequency of the collision process versus the particle radius are given as asterisks in Fig. 4(a). Theoretical models are indicated by different curves, where the Schulze[4] and Nguyen[6] literature models were initially developed for prediction of collision times (half of the reciprocal of the AE frequency). As can be seen, our model sits in between the other two models and gives the best match to the experimental data. The log–log plot clearly shows the general trend that the AE frequency decreases with the particle radius in a power law relationship. The frequency of AE is independent of the particle settling velocity V_t, which was unconstrained in these experiments. AE of data limited to 1.0 mm and 1.5 mm (bubble sizes) supports the view predicted by our model at the oscillation frequency independent of bubble size.

In Fig. 4(b), a comparison is presented of the experimental data and theoretical predictions on the maximum amplitude of the bubble–particle collision AE for a particle of radius 500 μm. The maximum deviation of the experimental values from the theoretical values predicted by our model is less than 100 mPa order over a 100 − 350 mPa maximum amplitude range. The plot of the AE amplitude variation with the distance of the hydrophone position from the bubble particle impact point demonstrates that the amplitude falls off as the $1/r$. This proves that the bubble particle collision can be regarded as a monopole source of acoustic emissions. To first order, the experimental results for maximum AE amplitude are independent of bubble size.

V. CONCLUSION

In this paper we theoretically and experimentally investigated the acoustic emissions during the collision interaction between a solid particle and a stationary gas bubble in a liquid for the first time. Analytical predictions for the frequency and maximum amplitude of the acoustic emissions caused by a collision are based on the following parameters, particle size and density, particle impact velocity, liquid density, and surface tension of the gas–liquid interface. With the current

experimental apparatus we can unambiguously identify the acoustic signature associated with the bubble–particle collision interaction. The experimental data show that the frequency and amplitude of the acoustic emissions have close correspondence with theoretically derived dependencies on the particle radius and particle settling velocity.

[1]A. V. Nguyen and H. J. Schulze, *Colloidal Science of Flotation* (CRC Press, Boca Raton, FL, 2003), Chaps. 10–11, 16.

[2]L. F. Evans, "Bubble-mineral attachment in flotation," Indust. Eng. Chem. **46**, 2420–2424 (1954).

[3]A. Scheludko, B. V. Toshev, and D. T. Bojadjiev, "Attachment of particles to a liquid surface (Capillary theory of flotation)," J. Chem. Soc., Faraday Trans. 1 **72**, 2815–2828 (1976).

[4]H. J. Schulze, B. Radoev, T. Geidel, H. Stechemesser, and E. Topfer, "Investigations of the collision process between particles and gas bubbles in flotation—A theoretical analysis," Int. J. Miner. Process. **27**, 263–278 (1989).

[5]Y. Ye and J. D. Miller, "The significance of bubble-particle contact time during collision in the analysis of flotation phenomena," Int. J. Miner. Process. **25**, 199–219 (1989).

[6]A. V. Nguyen, H. J. Schulze, H. Stechemesser, and G. Zobel, "Contact time during impact of a spherical particle against a plane gas–liquid interface: Theory," Int. J. Miner. Process. **50**, 97–111 (1997).

[7]H. Bergelt, H. Stechemesser, and K. Weber, "Experimental investigation of collision time of a spherical particle colliding with a liquid/gas interface," Int. J. Miner. Process. **34**, 321–331 (1992).

[8]A. V. Nguyen, H. J. Schulze, H. Stechemesser, and G. Zobel, "Contact time during impact of a spherical particle against a plane gas–liquid interface: Experiment," Int. J. Miner. Process. **50**, 113–125 (1997).

[9]G. Wierink, J. Tiitinen, and K. Heiskanen, "Mapping of collision regimes in flotation modeling," in *Seventh International Conference on CFD in the Minerals and Process Industries* (CSIRO, Melbourne, Australia, 2009), 5 pp.

[10]F. J. Bueche, *Introduction to Physics for Scientists and Engineers*, 3rd ed. (McGraw-Hill, New York, 1980), pp. 95.

[11]R. Serway and J. Jewett, *Physics for Scientists and Engineers* (Cengage Learning, Melbourne, Australia, 2009), pp. 451–453.

[12]D. F. James, "The meniscus on the outside of a small circular cylinder," J. Fluid Mech. **63**, 657–664 (1974).

[13]J. Billingham and A. C. King, *Wave Motion* (Cambridge University Press, Cambridge, UK, 2001), pp. 57–64.

[14]W. Wang, Z. Zhou, K. Nandakumar, Z. Xu, and J. H. Masliyah, "Attachment of individual particles to a stationary air bubble in model systems," Int. J. Miner. Process. **68**, 47–69 (2003).

[15]A. O. Maksimov and T. G. Leighton, "Transient processes near the acoustic threshold of parametrically-driven bubble shape oscillations," Acta Acust. **87**, 322–332 (2001).